Water gas shift reaction over Cu catalyst supported by mixed oxide materials for fuel cell application

Pannipa Tepamatr[1], Sumittra Charojrochkul[2] and Navadol Laosiripojana[1]

[1]*The Joint Graduate School of Energy and Environment, King Mongkut's University of Technology Thonburi, Bangkok, Thailand*
[2]*National Metal and Materials Technology Center, NSTDA, Pathumthani, Thailand*

Abstract. The water gas shift activities of Cu on ceria and Gd doped ceria have been studied for the further enhancement of hydrogen purity [1] after the steam reforming of ethanol. The catalytic properties of commercial catalysts were also studied to compare with the as-prepared catalysts. Copper-containing cerium oxide materials are shown in this work to be suitable for the high temperature. Copper-ceria is a stable high-temperature shift catalyst, unlike iron-chrome catalysts that deactivate severely in CO_2-rich gases. We found that 5%Cu/10%GDC(D) has much higher activity than other copper ceria based catalysts. The finely dispersed CuO species is favorable to the higher activity, which explained the activity enhancement of this catalyst. The kinetics of the WGS reaction over Cu catalysts supported by mixed oxide materials were measured in the temperature range 200-400 ℃. An independence of the CO conversion rate on CO_2 and H_2 was found.

1 Introduction

The water-gas shift (WGS) reaction ($CO + H_2O \leftrightarrow CO_2 + H_2$) plays an important role in fuel processing. For PEM fuel cell applications, novel low-temperature WGS catalysts are under development to upgrade the hydrogen-rich reformate gas streams where the catalyst possesses improved activity and greatly improved stability over the commercial Cu–ZnO catalysts [1,2]. The latter have been optimized for the production of chemicals, and are not suitable for fuel cell applications as they are pyrophoric and deactivate fast after exposure to air and/or water condensation. Because of its high activity [3] and low price, copper is still an excellent candidate as the active component of a new generation, stable catalyst for the WGS reaction. Many promising such catalyst compositions use ceria carriers, with the latter actively contributing to the making of an active and stable Cu-based catalyst.

As one of the most important rare earth oxides, ceria has been extensively applied in catalysis, electrochemistry, and optics, due to its unique physical and chemical properties. CeO2 retains its defective fluorite-type crystal structure during the oxygen storage and release processes, and thus is an active oxide component of various oxidation catalysts used in diverse redox catalytic reactions [4,5]. Ceria-based catalysts are very good WGS catalysts [6–9], and the Cu–CeO2 system was first reported by Li et al. as a promising low-temperature shift catalyst [6]. The choice of Cu–CeO2 for high-temperature WGS applications was also rationalized [9], because this copper-based system is more stable than the commercial Cu/ZnO. For a practical fuel cell system, operating under frequent shutdown and restart cycles, ceria needs to be modified by addition of zirconia [10] or another dopant to avoid formation of Ce(III) hydroxycarbonate during shutdown to RT in the water-containing reaction gas. Another approach is to regenerate the catalyst frequently by oxidation at 400–450 ^{o}C [10,11] or to run the reaction in oxygen-assisted mode [11]. Despite this issue, ceria and doped ceria remains the support of choice when a highly dispersed metal preparation is desired, which must remain stable over a wide temperature range [9]; and when surface oxygen availability to the metal is required, as in the case of the water-gas shift reaction [8].

During the last decade, copper–ceria catalysts have been widely studied for the WGS reaction via different approaches. Synthesis, structural and surface investigations by multiple characterization techniques, activity and stability tests, investigations of the reaction mechanism, and determination of the active sites have been addressed. For example, Wang et al. observed reversible redox properties of copper in $Ce_{1-x}Cu_xO_2$ by in situ XAFS and time-resolved XRD measurements [12], and further found a complex interaction between copper and the oxygen vacancies of ceria [13]. Koryabkina et al. found that the addition of ceria did not increase the WGS rate per unit of Cu surface area, and claimed that ceria is not a promoter for copper [14], while Djinovi ć et al. reported that the activity of CuO–CeO_2 catalysts for WGS reaction was related to the extent of surface CeO_2 reduction and the interaction between CuO and CeO_2 [15]. Thus, the basic questions regarding the structure–activity

relationship and the interaction of copper and ceria in the WGS reaction have been addressed, but often with divergent conclusions. In our opinion, a consensus must be reached soon to enable better catalyst designs and development of active and stable water-gas shift catalysts for practical fuel cell applications. This will potentially lead to novel, properly designed Cu-containing CeO_2 catalysts of comparable activity to the more expensive choices of Pt- or Au-based WGS catalysts.

In this work, we have studied different preparation methods to obtain the copper–ceria materials, developed a structural model for each sample, and attempted to correlate the catalyst activity to the presence or absence of certain Cu species and their interaction with the surface of ceria

2 Experimental Procedure

2.1 Catalysts Preparation

2.1.1 Preparation of Support

Cerium oxide and gadolinium doped ceria (GDC) were prepared by a combustion synthesis technique [16] using urea as a fuel. Nitrate salts of cerium ($Ce(NO_3)_3.6H_2O$, 99.5%, Alfa Aesar) and gadolinium ($Gd(NO_3)_3.6H_2O$, 99.9%, Alfa Aesar) were used as initial chemical reactants. The stoichiometry between metal nitrate and urea was 2.5:1.

Nitrate salts of cerium ($Ce(NO_3)_3.6H_2O$) and urea were mixed for the preparation of cerium oxide. The preparation of gadolinium doped ceria (GDC), $Ce(NO_3)_3.6H_2O$ and $Gd(NO_3)_3.6H_2O$ were mixed with urea as the desired ratio. A minimum amount of deionized water was added to the mixed reactant to obtain a homogenous solution. The crucible containing the mixed reactant was then heated using a Bunsen burner until an autoignition occurred. The catalytic properties of CeO_2 (AlfaAesar), CeO_2 (Nanophase), 10%gadolinia-doped ceria (Daiichi) and 10%gadolinia-doped ceria (FuelCellMaterials), which denoted as A, B, C and D, were also studied to compare with the as-prepared catalysts.

2.1.2 Preparation of Catalysts

Cu catalyst was prepared by impregnation method. Appropriate amount of $Cu(NO_3)_2.3H_2O$ was dissolved in minimal amount of deionized water. The salts solution was added to CeO_2 (Alfa Aesar), CeO_2 (Nanophase), 10%gadolinium doped ceria (GDC, FuelCellMaterials), 10%gadolinium doped ceria (GDC, Daiichi), CeO_2 (combustion) and 10%gadolinium doped ceria (combustion). All the catalysts were dried at 110 ℃ for 12 hours and then calcined in an oven at 650 ℃ for 8 hours.

2.2 Catalyst characterization

2.2.1 Standard characterization

Specific surface areas (m^2/g) and pore size distribution were determined by N_2 adsorption-desorption isotherms at 77.3 K using Quantachrome NOVA 1200e. The specific surface area of the sample was calculated following the Brunauer Emmett Teller (BET) procedure in the range of 0.05-0.3. Prior to the measurements, the samples were outgassed in vacuum at 300 ℃ for 6 hours.

The XRD diffractograms presented in this study were recorded employing nickel-filtered Cu K_α radiation (λ = 1.5406 Å) operating at 40 kV and the current was 40 mA. The analyses were carried out at 0.02° step and 0.5 s per step over a 2θ range of 20-80°.

2.2.2 Temperature Programmed Reduction

TPR experiments were performed under a flow of 5%H_2/95%Ar mixture over 0.05 g of catalyst from 40 ℃ to 1000 ℃ using a heating rate of 10°C/min. Prior to the measurement, the catalysts were treated under high purity helium gas at 120°C for 30 minutes. The amount of H_2 uptake during the reduction was measured by using a thermal conductivity detector. The curves in H_2-TPR profile correspond to H_2 consumption.

2.2.3 Scanning electron microscopy (SEM)

SEM images were taken on a FE-SEM)HITACHI SU-8030(with high vacuum mode using secondary electrons and an acceleration tension of 30 kV. Samples were analyzed by spreading them on a carbon tape. Energy dispersive X-ray spectroscopy (EDX) was used in connection with SEM for the elemental analysis. The elemental mapping was also collected with the same spectrophotometer.

2.3 Reaction testing

An amount of 150 mg catalyst was loaded between two layers of quartz wool in a stainless-steel fixed bed flow reactor. The reactor was placed inside a tube furnace. The flow of feed gases was controlled by mass flow controllers)Aalborg(. The initial feed gas of CO and N_2 was mixed with water vapour which was controlled by using a syringe pump. The mixed feed gas composition 5% CO, 10% H_2O, balanced in N_2 and total flow rate was 100 ml/min, was passed through the catalyst bed in the reactor. The temperature of catalysts was increased from 100 ℃ up to 500 ℃. The column utilized in the chromatograph was a Unibead C, 15 m × 0.53 mm stainless-steel packed column. The outlet gasses were analyzed by using an on-line gas chromatography (Shimadzu GC-14B) equipped with a TCD analyzer. The catalytic activities were calculated by using equation [1]:

$$\%COconversion = \frac{CO_{in} - CO_{out}}{CO_{in}} \times 100 \quad (1)$$

3. Result and Discussion

3.1 Characterization of monometallic Cu catalysts

XRD patterns of supports and Cu catalysts are presented in Fig. 1. All samples exhibit the diffraction peaks which

correspond to the fluorite structure of CeO_2. Copper oxide is not observed in all samples as there are only 5% of Cu in each sample. Based on Bragg's equation, the lattice parameters of ceria and doped catalysts were calculated from (1 1 1) crystallographic planes. For pure CeO_2 support, the lattice parameter is found to be 0.541 nm which is in agreement with other works [17,18]. The lattice parameter of other catalysts (Cu/CeO_2 and Cu/GDC) also displayed similar values in the range of 0.0545–0.0547 nm. From these results, it can be concluded that an addition of Cu did not lead to a significant modification of the ceria bulk structure.

Tables 1 and 2 summarize the results from particle analyses and XRD. Lowering of the surface area and increasing of crystallite size of Cu catalysts are believed to be a consequence of sintering at high temperature. The % metal dispersion data indicate that Cu metal can be better dispersed in GDC (C), GDC (D) and CeO_2 (combustion). However, the dispersion of $5\%Cu/CeO_2$ (A) cannot be detected. This result was due to agglomeration and the growth of metal–ceria crystallites.

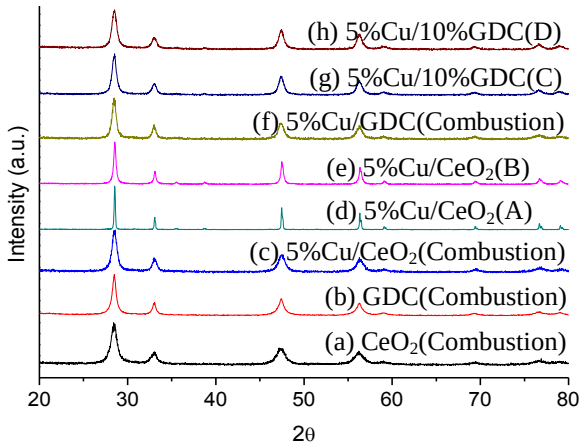

Figure 1. XRD patterns of supports and Cu catalysts.

Table 1. Standard characterization of supports.

Catalysts	Crystallite size (nm)	BET surface area (m^2/g)
CeO_2 (A)	42.27	6.600
CeO_2 (B)	30.60	52.30
GDC (C)	12.26	85.53
GDC (D)	4.540	192.8
CeO_2 (Combustion)	10.15	66.47
GDC (Combustion)	11.02	33.57

Table 2. Standard characterization of Cu catalysts.

Catalysts	Crystallite size (nm)	BET surface area m^2/g	% dispersion
$5\%Cu/CeO_2$ (A)	66.67	1.158	-
$5\%Cu/CeO_2$ (B)	30.04	26.45	11
5%Cu/GDC (C)	14.24	45.61	25
5%Cu/GDC (D)	12.75	41.93	32
$5\%Cu/CeO_2$ (Combustion)	12.52	39.67	31
5%Cu/GDC (Combustion)	15.21	21.01	21

Figure 2 shows H_2-TPR profiles of Cu on various supports. The reduction temperature of all samples is observed at temperature lower than 400 ^oC. The 5%Cu/10%GDC (C) and 5%Cu/10%GDC (D) catalysts have three reduction peaks at about 150 ^oC, 180 ^oC and 200 ^oC which are denoted as peaks β, γ and δ, respectively. The peaks β, γ and δ assigned to finely dispersed CuO [19,20], the reduction of Cu^{2+} ions in the Cu-O-Ce solid solution [21,22], and bulk CuO particles [23-25], respectively. In case of 5%Cu/10%GDC(D), the peaks β, γ and δ are slightly shifted to lower temperatures compared to 5%Cu/10%GDC(C). The H_2-TPR profiles of $5\%Cu/CeO_2$(B) and $5\%Cu/CeO_2$(combustion) exhibit two reduction peaks at about 140 ^oC, and 200 ^oC. The first peak appearing at about 140 ^oC, denoted as peak α, is attributed to the reduction of non-crystalline copper oxide in close contact with ceria. The second sharp peak is assigned to the reduction of Cu^{2+} ions in the Cu-O-Ce solid solution. The reduction of CuO species interacting with CeO_2 of $5\%Cu/CeO_2$(B) catalyst is easier than that of $5\%Cu/CeO_2$(combustion). For 5%Cu/10%GDC (combustion), only one reduction peak at high temperature corresponding to Cu^{2+} ions in the Cu-O-Ce solid solution was observed. Moreover, in the case of 5%Cu/CeO2(A), the peak β disappeared while H_2 reduction peak corresponding to the reduction of Cu^{2+} ions in the Cu-O-Ce solution and reduction of bulk CuO particles shift to higher temperatures. Interestingly, the reduction of Cu^{2+} ions in the Cu-O-Ce solid solution of 5%Cu/10%GDC(D) is easier than that of other catalysts. It is expected that the easier reducibility of catalyst resulting in higher CO conversion.

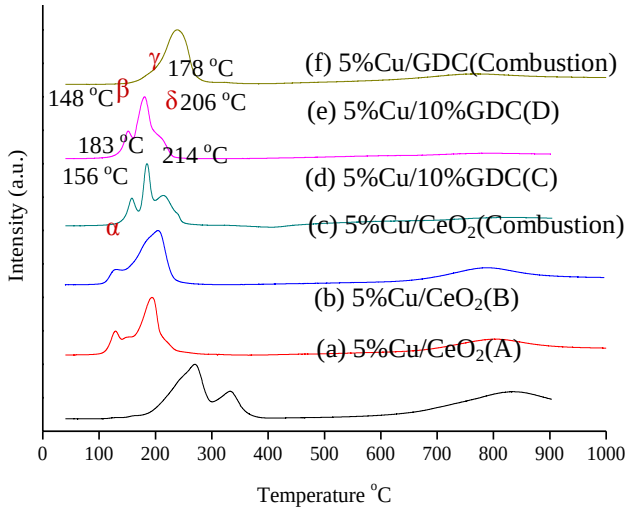

Figure 2. H_2-TPR profiles of Cu on various supports.

3.2 Water gas shift activity of monometallic Cu catalysts

Fig. 3 shows activities of Cu on commercial CeO_2 and GDC mixed oxide. It appears that 5%Cu/CeO_2(A) and 5%Cu/CeO_2(B) have weak WGS activity and start to convert CO to CO_2 at temperature above 150 ℃. The activity of 5%Cu/CeO_2(B) is slightly higher than that of 5%Cu/CeO_2(A). Cu catalysts on GDC(C) and GDC(D) were more drastically active than Cu catalysts on ceria. The CO conversion of 5%Cu/10%GDC(D) starts above 100°C and rises up quickly to reach the maximum of 80 %conversion at about 400°C. Above 400°C, the activity reaches equilibrium and slightly declines. The activities of 5%Cu/10%GDC(D) are drastically higher than the activity of 5%Cu/10%GDC(C). For 5%Cu/GDC(C) the conversion started above 100°C and rises up to reach the maximum of 75%conversion at 500°C.

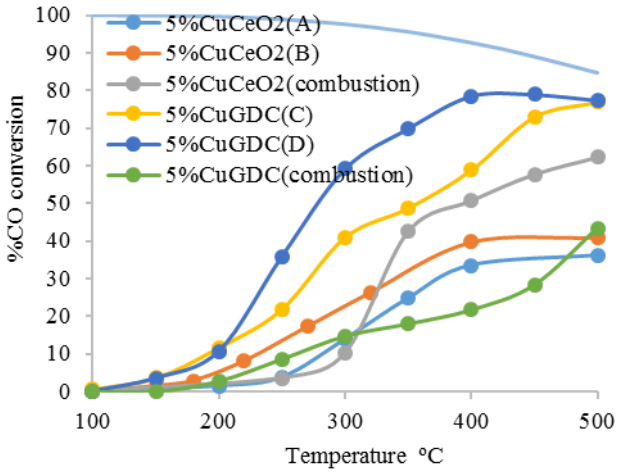

Figure 3. WGS catalytic activity of Cu catalyst on various support.

Catalytic activities of Cu on CeO_2 and GDC prepared by a combustion synthesis technique are also studied. It can be seen that 5%Cu/CeO_2**(**combustion**)** is not an active catalyst for WGS reaction. A modification of ceria with Gd drastically decreased the activity for WGS reaction. The order of activity at 500°C is that 5%Cu/10%GDC**(**D**)** > 5%Cu/10%GDC**(**C**)** > 5%Cu/CeO_2**(**combustion**)** > 5%Cu/CeO_2**(**B**)** ~ 5%Cu/CeO_2**(**A**)** ~ 5%Cu/10%GDC**(**combustion**)**. For 5%Cu/CeO_2**(**A**)**, there is a drastic fall in the activity compared with other catalyst due to the reduction peak corresponding to finely dispersed CuO disappear. An additional peak assigned to bulk CuO particles is observed at high temperature. Therefore, the TPR results directly evidenced that the finely dispersed CuO species is more efficient as active sites for WGS reaction. The formation of bulk CuO species is not beneficial for the activity. The finely dispersed CuO species supported on smaller CeO_2 is favorable to the higher activity.

4 Conclusion

The catalytic activities of Cu catalyst on ceria based supports have been studied. It was found that 5%Cu/10%GDC(D) yields the highest catalytic activity. 5%Cu/10%GDC(D) reaches the maximum of 80% conversion at about 400°C. Various evidences seemed to point to the direction that the enhanced catalytic activity of Cu on mixed oxide support was mainly governed by reducibility. The TPR results directly evidenced that the finely dispersed CuO species is more favorable to the higher activity. . The formation of bulk CuO species is not beneficial for the activity.

References

1. D.S. Newsome, Catal. Rev. Sci. Eng. **21**, 275 (1980).
2. C. Rhodes, G.J. Hutchings, A.M. Ward, Catal. Today **23**, 43 (1995).
3. M. Mavrikakis, A.A. Gokhale, J.A. Dumesic, J. Am. Chem. Soc. **130**, 1402 (2008).
4. J.L.G. Fierro, J. Soria, J. Sanz, J.M. Rojo, J. Solid State Chem. **66**, 154 (1987).
5. C. Padeste, N.W. Cant, D.L. Trimm, Catal. Lett. **18**, 305 (1993).
6. Y. Li, Q. Fu, M. Flytzani-Stephanopoulos, Appl. Catal. B **27**, 179 (2000).
7. Q. Fu, A. Weber, M. Flytzani-Stephanopoulos, Catal. Lett. **77**, 187 (2001).
8. Q. Fu, H. Saltsburg, M. Flytzani-Stephanopoulos, Science **301**, 935 (2003).
9. X. Qi, M. Flytzani-Stephanopoulos, Ind. Eng. Chem. Res. **43**, 3055 (2004).
10. W. Ruettinger, X. Liu, R.J. Farrauto, Appl. Catal. B **65**, 135 (2006).
11. W. Deng, M. Flytzani-Stephanopoulos, Angew. Chem. Int. Ed. **45**, 2285 (2006).
12. X. Wang, J.A. Rodriguez, J.C. Hanson, D. Gamarra, M. Fernandez-Garcia, A. Martinez-Arias, J. Phys. Chem. B **109**, 19595 (2005).

13. X. Wang, J.A. Rodriguez, J.C. Hanson, D. Gamarra, A. Martinez-Arias, M. Fernandez-Garcia, J. Phys. Chem. B **110**, 428 (2006).
14. N.A. Koryabkina, A.A. Phatak, W.F. Ruettinger, R.J. Farrauto, F.H. Ribeiro, J. Catal. **217**, 233 (2003).
15. P. Djinovi´c, J. Batista, A. Pintar, Appl. Catal. A **347**, 23 (2008).
16. S. Charojrochkul, W. Nualpaeng, N. Laosiripojana, S. Assabumrungrat, *Materials Challenge and testing for Supply of Energy and Resources*, Springer.
17. P. Panagiotopoulou, J. Papavasiliou, G. Avgouropoulos, T. Ioannides, D.I. Kondarides, Chem. Eng. J., **134**, 16 (2007).
18. Q. Fu, W. Deng, H. Saltsburg, M. Flytzani-Stephanopoulos, M., Appl. Catal. B: Environ., **56**, 57 (2005).
19. X. Tang, B. Zhang, Y. Li, Y. Xu, Q. Xin, W. Shen, Applied Catalysis A General **190**, 25 (2000).
20. 20. H. Yahiro, K. Murawaki, K. Saiki, T. Yamamoto, H. Yamaura, Catal Today **126**, 436 (2007).
21. M.F. Luo, J.M. Ma, J.Q. Lu, Y.P. Song, Y.J. Wang, Journal of Catalysis **246**, 52 (2007).
22. G. Avgouropoulos, T. Ioannides, Applied Catalysis A General **244**, 155 (2003)**.**
23. J.F. Chen, Y.Y. Zhan, J.J. Zhu, C.Q. Chen, X.Y. Lin, Q. Zheng. Applied Catalysis A General **377**, 121 (2010).
24. X. Zheng, X. Zhang, X. Wang, S. Wang, S. Wu, Applied Catalysis A: General **295**, 142 (2005).
25. L.J. Kundakovic, M.F. Stephanopoulos, Applied Catalysis A: General **171**, 13 (1998).